Synthesis of Nested Coaxial Multiple-Walled Nanotubes by Atomic Layer Deposition

Diefeng Gu,[†,‡] Helmut Baumgart,[†,‡,*] Tarek M. Abdel-Fattah,[‡,§] and Gon Namkoong[†,‡]

[†]Department of Electrical Engineering, Old Dominion University, Norfolk, Virginia 23529, [‡]The Applied Research Center, CNU&ODU, Jefferson Lab, Newport News, Virginia 23606, and [§]Department of Biology Chemistry and Environmental Science, Christopher Newport University, Newport News, Virginia 23606

ABSTRACT Nested multiple-walled coaxial nanotube structures of transition metal oxides, semiconductors, and metals were successfully synthesized by atomic layer deposition (ALD) techniques utilizing nanoporous anodic aluminum oxide (AAO) as templates. In order to fabricate free-standing tube-in-tube nanostructures, successive ALD nanotubes were grown on the interior template walls of the AAO nanochannels. The coaxial nanotubes were alternated by sacrificial spacers of ALD Al_2O_3, to be chemically removed to release the nanotubes from the AAO template. In this study, we synthesized a novel nanostructure with up to five nested coaxial nanotubes within AAO templates. This synthesis can be extended to fabricate *n*-times tube-in-tube nanostructures of different materials with applications in multisensors, broadband detectors, nanocapacitors, and photovoltaic cells.

KEYWORDS: atomic layer deposition · nested multiple-walled coaxial nanotubes · coaxial sacrificial spacer layer · porous alumina templates · chemical nanotube release

Porous anodic aluminum oxide (AAO) templates are increasingly finding many applications in sensors due to its high-density nanopores with increased surface area, in photonic crystals,[1] and in electro-osmotic pumps for liquid-based nanoscale separations.[2] AAO and other nanoporous materials are very attractive as a template for cost-saving and very efficient nanofabrication.[3−6] AAO is formed by electrochemical oxidation of aluminum in acidic solutions to form regular porous channels.[7−9] The diameter of the pore depends on the electrolyte nature, its temperature and concentration, the current density, and other parameters of the anodization process.[7−11]

However, current existing technology in AAO templates produces very simple nanostructures such as single nanorod or nanotube structures which limit their available surface area or functionalities.[12,13] Recently, several attempts at double-walled nanotubes were reported using sol−gel methods and electrochemical deposition within AAO, which only offer limited control of there parameters such as nanotube size, diameter, thickness, and spacing between nanotubes.[14−17]

In addition, AAO templates can be applied to various materials to increase their functionality. For example, hafnium oxide (HfO_2), zirconium oxide (ZrO_2), and zinc oxide (ZnO) tubes, with high aspect ratio and a small size of nanotubes or nanowires, are expected to improve the sensitivity of chemical sensors and to reinforce thermal stability and toughness of the materials analogous to carbon nanotubes.[18] In this study, we expand the potential applications of AAO templates by utilizing atomic layer deposition (ALD) to create far more complex nested multiple-walled nanostructures within AAO templates. Atomic layer deposition is a thin film growth technology based on a sequence of two self-limiting reactions between gaseous precursor molecules and a solid surface to deposit films in a layer-by-layer with atomic resolution. Since gas phase reactants are utilized, conformal coatings can be achieved with very high aspect ratio geometries on three-dimensional (3D) porous structures. Such template-guided, conformal depositions by ALD can produce concentric nested multilayered nanotubes and thus enable the fabrication of multilayered nanotube architectures inside the nanopore templates. In this paper, we report for the first time the synthesis of novel highly ordered multiple-walled tube-in-tube nanostructures with up to five nested coaxial nanotubes embedded in AAO templates. This template-guided ALD technique also allows for remarkable control of nanotube thickness, diameter, and spacing within atomic resolution. Therefore, our newly developed technique can be readily extended to synthesize *n*-times nested multiwalled nanostructures of

*Address correspondence to hbaumgar@odu.edu.

Received for review September 18, 2009 and accepted January 7, 2010.

Published online January 19, 2010.
10.1021/nn901250w

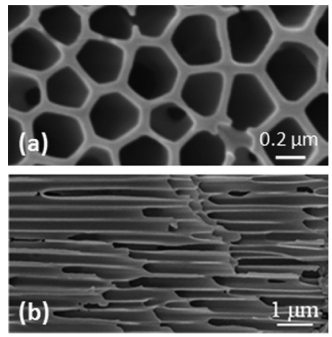

Figure 1. (a) SEM micrograph top view of the nanopore structure of an AAO template with polished surface by ion milling, and (b) cross-sectional SEM micrograph of a cleavage site through an AAO template revealing the smooth surface morphology of the straight nanopores.

different materials for numerous applications including chemical and biosensors, broadband detectors, nanocapacitors, and photovoltaic devices. It is noteworthy that the benefit derived from the tube-in-tube concept for sensor applications lies in the dramatic increase of the reactive surface area. Already, the simplest case of a double-walled nanotube of metal oxides will increase the reactive surface area at least four times, which renders these nested tube-in-tube nanostructures very attractive in multisensing capability. Furthermore, we can expand this process strategy for building multiwalled nanotubes of different metal oxide materials for sensing complex multianalytes. Broadband sensing capabilities can be engineered by substituting a specific sensor material for one of the multiple tubes and alternating the remaining tube material to target different chemicals for detection.

RESULTS AND DISCUSSION

Figure 1a shows a representative SEM image of the pore structure of the AAO after the surface was planarized by ion milling. The pore size is in the range of 200−300 nm, and the wall width between pores is around 50 nm. The cross-sectional SEM image of Figure 1b confirms that the pores are all parallel to each other and extend across the whole template thickness of 60 μm. Figure 1b demonstrates the excellent surface finish of the inner pore walls of the template that is critical for obtaining highly ordered tube-in-tube nanostructures because our ALD thin film coating techniques replicate the surface finish on an angstrom scale. High quality internal interfaces are required to reproducibly grow nested films by ALD.

As a first step, we successfully fabricated single nanotubes of insulating ZrO_2, semiconducting ZnO, and metallic Pt by conformally coating the inside walls of the AAO nanopores. Figure 2a shows an SEM micrograph of partially released single-walled ZrO_2 nanotubes. Figure 2b shows SEM views of cleavage sample of partially released single ZnO nanotubes, and Figure 2c shows again a cleaved sample of partially released

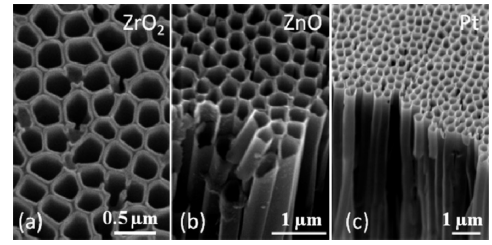

Figure 2. SEM images of free-standing single-walled nanotubes (a) ALD synthesized nanotubes of insulating high-*k* ZrO_2; (b) ALD synthesized nanotubes of semiconducting ZnO; (c) ALD synthesized metallic Pt nanotubes.

single Pt nanotubes, which were obtained by dissolving the alumina template in NaOH solution. In our previous work, energy-dispersive X-ray spectroscopy (EDS) mapping of the cross-sectional AAO template coated with ZrO_2 and ZnO proved that the characteristic X-ray signal of Zr and Zn is uniformly distributed across the entire length of 60 μm of the AAO pores.[10] Our EDS analysis confirms that ALD allows for thin film conformity on complex patterned surface topographies with high aspect ratio and atomic level control of film composition and film thickness. The length and diameter of ZrO_2 nanotubes are dependent upon the pore length of the AAO template, the pore diameter, and the optimized ALD deposition conditions.[10,11] Utilizing (trimethyl)methylcyclopentadienyl platinum ($MeCpPtMe_3$) as precursor for ALD Pt deposition, we found that the depth penetration into the nanoporous template saturates at around 15 μm from the surface even with exposure times exceeding 30 s. This is attributed to the combined effects of AAO pore size and the ($MeCpPtMe_3$) precursor diffusion rate, which is inversely proportional to the square root of the molecular weight for this Pt precursor.[19]

Figure 2 indicates there is plenty of space inside the single-walled nanotubes within the AAO template for additional nanotubes to be grown by ALD. In the next process step, we utilized the first single-walled nanotube as the template surface for subsequent nested ALD film growth. Therefore, we can extend the synthesis into multilayered tube-in-tube structures by successively growing a second and third coaxial nanotube each with smaller dimensions inside the predecessor nanotube.

It is not technically feasible to grow free-standing nested coaxial nanotube structures by ALD. Instead, atomic layer deposition requires a solid surface to grow specific films layer-by-layer. The tube-in-tube structure can be achieved by successively growing a second and third coaxial tube each with smaller dimensions inside of the predecessor startup nanotube. For our fabrication strategy, we devised a sacrificial spacer process separating the active coaxial nanotubes during ALD film deposition. In order to fabricate such multiple-walled tube-in-tube structure using the ALD template method, two layers of 15 nm HfO_2 films were deposited

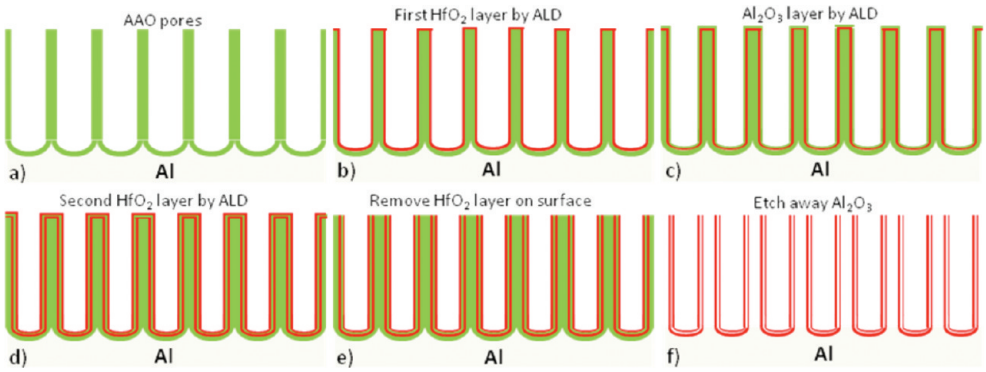

Figure 3. Schematic depiction of process sequence to synthesize free-standing HfO_2 nested coaxial tube-in-tube nanostructures: (a) start with fabrication of nanoporous AAO template, (b) first coating of inner pore walls with HfO_2 by ALD, (c) ALD deposition of sacrificial spacer layer consisting of Al_2O_3, (d) second coating of ALD HfO_2 layer on top of sacrificial spacer layer, (e) sputter removal of the ALD composite layers from surface of the AAO template in order to expose the sacrificial spacer layer and the AAO template walls, (f) releasing and separating the coaxial HfO_2 nanotubes by chemical dissolution of the alumina AAO template walls and the sacrificial ALD Al_2O_3 spacer layers in aqueous NaOH solution.

inside of the AAO pores, separated by 25 nm of Al_2O_3. The details of our fabrication strategy are shown in the two-dimensional schematic drawing of Figure 3a−f, using HfO_2 as an example. The reason for choosing to grow ALD Al_2O_3 nested nanotubes as sacrificial spacers is compelling. ALD Al_2O_3 constitutes chemically the same material as the alumina template, and thus both the sacrificial spacer and the remaining alumina template wall structure can be simultaneously removed by 1 M NaOH solution to separate the nested coaxial nanotubes. Following the ALD deposition of the three layers, the sample surface was again polished by ion milling to expose the surfaces of AAO and ALD grown alumina spacer to NaOH solution, as depicted in Figure 3e.

Figure 4a clearly confirms that a free-standing double-walled HfO_2 tube-in-tube structure was synthesized after removing the AAO template and the sacrificial spacer. The dimension of the spacer gap between the two active nanotubes can be engineered with the precise control in the angstrom range over layer thickness afforded by ALD. The free-standing nanotube array is schematically depicted in Figure 4b, generalizing the concept of coaxial nanotubes with completely exposed inner and outer surface areas. Such multilayered nanotubes can find many applications in biosensors and chemical detectors, which benefit from the increased surface area of the nested nanotube detector material interacting with the environment. Therefore, coaxially nested nanotube structures with exposed surfaces offer a considerable advantage over nanorods in terms of area available for surface reactions.

Another key requirement for our fabrication method is the subsequently completed exposure of the surfaces of the coaxial nanotube structures by wet chemical release procedures. While sodium hydroxide (NaOH) solution is the preferred means to dissolve the AAO template, the dissolution process needs to be optimized for the various materials. Various process parameters and etch chemistry characteristics responsible for the releases of ALD ZnO nanotubes from AAO templates were investigated. We observed that the etch chemistry of aqueous NaOH solution exhibits insufficient selectivity between the Al_2O_3 template and the ALD ZnO nanotubes. Figure 5a presents the thermodynamic modeling diagram showing the distributions of the fraction of all Al^{3+} species at different pH values calculated at 298 K for 0.001 mM Al^{3+} solution. The formation of solid alumina is in the pH range of 4.2 to 9.8, and the maximum solubility of Al_2O_3 is at pH below 4.2 and above pH 9.8. The thermodynamic modeling diagram of Figure 5b shows the distributions of the fraction of all Zn^{2+} species at different pH values calculated at 298 K for 0.001 mM Zn^{2+} solution. The thermody-

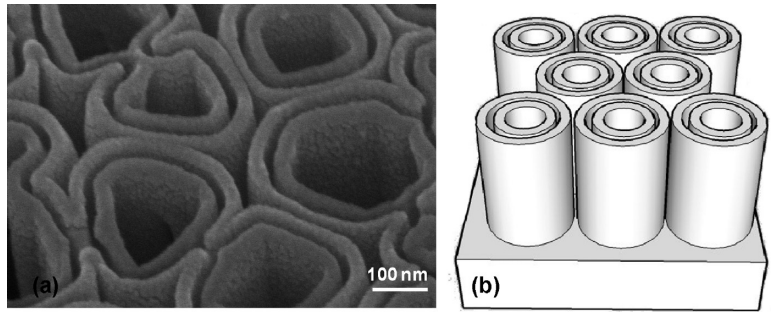

Figure 4. (a) High-magnification tilted SEM top view of resultant coaxial HfO_2 nanotubes following release from the AAO template and removing the sacrificial spacer Al_2O_3 layer to expose both the inner and outer surfaces of the nested nanotubes. (b) Schematic model highlighting the design of arrays of free-standing coaxial nested nanotubes.

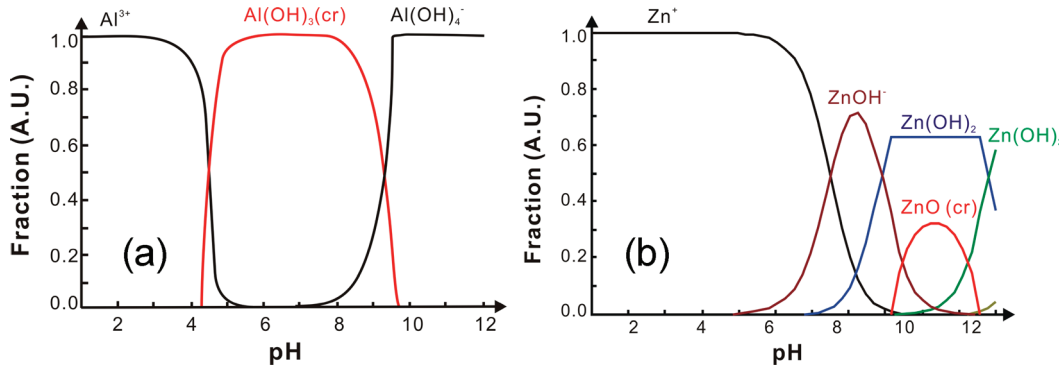

Figure 5. Thermodynamic modeling diagram showing the distributions of the fraction (a) Al^{3+} species *vs* pH, (b) Zn^{2+} species *vs* pH.

namic modeling indicates that zinc always has soluble species at any pH value. The existence of crystalline ZnO is in the pH range of 9.2 to 11.5. The maximum solubility of crystalline ZnO is at pH below 9.2 and above pH 11.5, which explains why NaOH solution at pH 13 partially etched and degraded the ZnO surface. On the basis of the thermodynamic modeling work, a buffered NaOH etch solution in the range of pH 10.3−11.0 was implemented to remedy these challenges. Experimentally, pH 11 was used to successfully remove AAO (Figure 2b).

In the example of Figure 4, there was only partial release from the AAO template, where the nested coaxial nanotubes are still attached to the substrate, leaving them free-standing in upright position. For many practical applications, the embedded nanotubes have to be released by removal of the AAO template in order to collect and to incorporate the resultant nanotubes in device structures. Certain applications call for attached upright standing coaxial nanotubes, while other applications require completely chemically released and detached coaxial nanotube structures. Figure 6 demonstrates that we can harvest by sonication large numbers of completely detached individual nanotubes with high aspect ratios of 300 and above.

Figure 7a displays a transmission electron microscopy (TEM) image of randomly dispersed HfO_2 nanotubes after release from the template and separation by sonication, while Figure 7b shows a high-magnification view of a single nested coaxial HfO_2 nanotube. With extended exposure time during ALD process, the length of HfO_2 tube-in-tube nanostructures of 50 μm can be achieved as seen in Figure 6, which corresponds to the AAO template thickness. The release of the nanotubes and complete detachment from the AAO template create opportunities for medical applications. Coaxial nanotube assembly of ALD ZrO_2 is extremely hard and durable ceramic nanotubes that cannot easily be machined by conventional techniques to these accurate dimensions on the nanoscale. These hard ceramic nanotubes could find applications as durable pipet tips in medical research and could serve various other functions in medical catheters or stents.

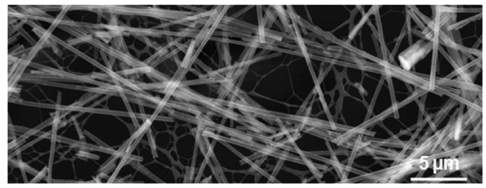

Figure 6. SEM micrograph showing large numbers of high aspect ratios coaxial ALD HfO_2 nanotubes after dissolving AAO template in NaOH solution. Subsequent sonication completely separates the ALD nanotubes for use in device applications.

The application potential becomes evident in Figure 7b, which displays the TEM image of the HfO_2 coaxial structure revealing minute details of the smooth morphology of the outer tube and the inner nested nanotube wall. The TEM images show a diameter of approximately 300 nm for the inner nanotube. However, the tube diameter can be custom tailored and continuously shrunk for the envisioned application by modulating the two-step anodization fabrication process for the AAO template.

Figures 4 and 7 demonstrate that there remains sufficient space inside the two nested coaxial nanotubes to continue our process of growing additional nanotubes by the ALD technique. In principle, our process of synthesis and assembly of nested multiple tube-in-tube nanostructures can be extended to *n*-layers. The only limitation is the initial diameter of the pores of the template and the thickness of the individual coaxial ALD nanotube layers. Since ALD growth affords superior layer thickness control in the angstrom range, these parameters can be modulated over a wide range, thus allowing the number of *n* nanotube layers that can be experimentally achieved to be adjustable at will. A demonstration of the technical feasibility of fabricating up to *n*-times nested nanotubes is provided by the SEM micrograph of Figure 8. In this top-down SEM image, we show a total number of five nested coaxial nanotube structures. With a reduction of the thickness of the nanotube walls, we can easily increase the number of nested nanotubes. Using various ALD processes, we have coated the interior walls of nanoporous templates with insulating transition metal oxide layers, electri-

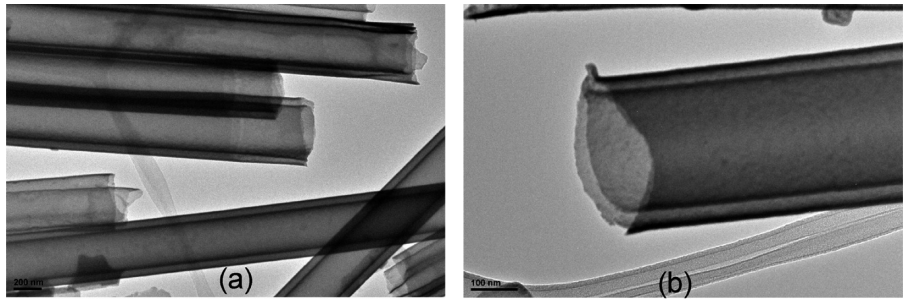

Figure 7. (a) TEM micrograph of several chemically released and separated coaxial HfO_2 nantubes. (b) High-magnification TEM image of a single tube-in-tube clearly showing the coaxial double-wall structure of released individual HfO_2 tube-in-tube structures.

cally conducting layers, and semiconducting layers such as ZnO and TiO_2. Such ALD semiconducting nanotubes can be alternated with electrically conducting tubes or insulating tubes, thereby offering intriguing possibilities for novel device architectures in the area of photovoltaics and other applications. Our process strategy of template-based ALD with sacrificial spacers is a powerful and very versatile fabrication technique because we can change at will the material type and the sequence of the nested coaxial multiple nanotubes. This flexibility to alternate between insulating, semiconducting, or conducting nested nanotubes will meet the requirements of many diverse device architectures.

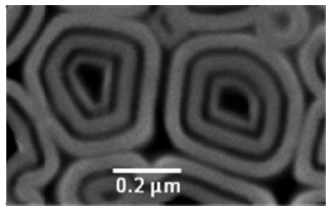

Figure 8. Top view SEM micrograph illustrating five nested coaxial ALD layers consisting of triple coaxial HfO_2 nanotubes separated by a gap and two sacrificial ALD Al_2O_3 spacer layers.

CONCLUSIONS

Multiple-walled coaxial nanotubes of five nested layers were successfully fabricated by the template replication method using ALD thin film technology. We have demonstrated nested coaxial nanotubes with the ability of alternating different materials such as insulating transition metal oxides, semiconductors, and metals using template synthesis technique. Subsequently, we have released and detached the nanotubes in order to expose their surfaces for potential sensing and detector applications. For this purpose, a sacrificial spacer process was developed. The resultant coaxial nanotube structures are highly ordered and absolutely conformal with the template pore structure and can achieve very high aspect ratios of 300 and above. This template-driven ALD technique for the fabrication of multiple tube-in-tube structures is not restricted to porous AAO templates but can be extended to polycarbonate nanoporous membranes, as well. Alternating different materials in the nested nanotube assembly enable custom design of broadband sensors and detectors and present application potentials in photovoltaics and for medical research.

EXPERIMENTAL SECTION

The AAO template was prepared by a two-step anodization procedure. After annealing high purity (99.999%) aluminum foil at 500 °C in a quartz furnace tube for 3 h under the constant flow of nitrogen, electrochemical polishing was performed to produce a smooth surface. After electrically polishing the Al foil, anodization was performed in 0.2 M oxalic acid at room temperature with an applied voltage for several hours. Higher voltage than 40 V was applied to control the pore size of anodic aluminum oxides (AAO), resulting in pore diameters of a few hundred nanometers.[20] The AAO substrates were subsequently transferred to the ALD reaction chamber in order to grow nested multiple-walled nanotubes within the AAO pores. In this work, we established the ALD process for Pt as a representative for metal nanotubes and ZnO and TiO_2 representing semiconducting metal oxide nanotubes. For the example of insulating materials, we utilized the transition metal oxides of ZrO_2, HfO_2, and Al_2O_3. ALD is a thin film growth technique that requires the sequential exposure of the sample to two chemical precursors to saturate the sample surface and to react with each other.[21,22] The technical details of the ALD process conditions and the different chemical precursors and deposition parameters utilized for all of the nested nanotubes investigated in this study are listed in Table 1.[10,11,23]

TABLE 1. Chemical Precursors and Deposition Parameters for the ALD Process

materials	deposition temp (°C)	precursor I	precursor II	growth rate (Å/cycle)
ZrO_2	250	tetrakis(dimethylamido)zirconium	H_2O vapor	1
ZnO	150	diethyl zinc	H_2O vapor	2.3
Pt	300	(trimethyl)methylcyclopentadienyl platinum	oxygen	0.5
TiO_2	250	titanium isopropoxide	H_2O vapor	0.3−0.4
HfO_2	250	tetrakis(dimethylamido)hafnium	H_2O vapor	1
Al_2O_3	300	trimethylaluminum	H_2O vapor	1

Following the ALD deposition of the aforementioned materials, the AAO sample surfaces were polished by ion milling to expose the template surface and the ALD grown alumina spacer to the NaOH solution. A 1 M NaOH solution was used to etch alu-

mina for all ALD nanotube materials except for ZnO nanotubes. For the case of ZnO, 0.1 M NaOH was used to achieve etching of the alumina template while minimizing the etch attack of the ZnO nanotubes. It is also essential to perform a post-ALD deposition annealing procedure for ZnO nanotubes at 600 °C for 10 min in air, in order to obtain high quality smooth surface morphologies of the ZnO nanotubes.

The TEM micrographs were recorded with JEOL 2100F model and SEM micrographs were obtained with JEOL JSM 6060 LV.

REFERENCES AND NOTES

1. Wang, B.; Fei, G. T.; Wang, M.; Kong, M. G.; De Zhang, L. Preparation of Photonic Crystals Made of Air Pores in Anodic Alumina. *Nanotechnology* **2007**, *18*, 365601.
2. Chen, W.; Yuan, J.-H.; Xia, X.-H. Characterization and Manipulation of the Electroosmotic Flow in Porous Anodic Alumina Membranes. *Anal. Chem.* **2005**, *77*, 8102–8108.
3. Fan, R.; Wu, Y.; Li, D; Yue, M.; Majumdar, A.; Yang, P. Fabrication of Silica Nanotube Arrays from Vertical Silicon Nanowire Templates. *J. Am. Chem. Soc.* **2003**, *125*, 5254–5255.
4. Zhao, Y.; Guo, Y.-G.; Zhang, Y.-L.; Jiao, K. Fabrication and Characterization of Highly Ordered Pt Nanotubule Arrays. *Phys. Chem. Chem. Phys.* **2004**, *6*, 1766–1768.
5. Lai, M.; Martinez, J. A. G.; Grätzel, M.; Riley, D. J. Preparation of Tin Dioxide Nanotubes *via* Electrosynthesis in a Template. *J. Mater. Chem.* **2006**, *16*, 2843–2845.
6. Steinhart, M.; Wendorff, J. H.; Greiner, A.; Wehrspohn, R. B.; Nielsch, K.; Schilling, J.; Choi, J.; Gösele, U. Polymer Nanotubes by Wetting of Ordered Porous Templates. *Science* **2002**, *14*, 1997.
7. Masuda, H.; Fukuda, K. Ordered Metal Nanohole Arrays Made by a 2-Step Replication of Honeycomb Structures of Anodic Alumina. *Science* **1995**, *268*, 1466–1469.
8. Menon, V. P.; Martin, C. R. Fabrication and Evaluation of Nanoelectrode Ensembles. *Anal. Chem.* **1995**, *67*, 1920–1928.
9. Cameron, M. A.; Gartland, I. P.; Smith, J. A.; Diaz, S. F.; George, S. M. Atomic Layer Deposition of SiO_2 and TiO_2 in Alumina Tubular Membranes: Pore Reduction and Effect of Surface Species on Gas Transport. *Langmuir* **2000**, *16*, 7435–7444.
10. Gu, D.; Baumgart, H.; Namkoong, G.; Abdel-Fattah, T. Atomic Layer Deposition of ZrO_2 and HfO_2 Nanotubes by Template Replication. *Electrochem. Solid-State Lett.* **2009**, *12*, K25–K28.
11. Abdel-Fattah, T.; Gu, D.; Baumgart, H.; Namkoong, G. Synthesis of Zirconia and Hafnia Nanotubes by Atomic Layer Deposition (ALD) Template Method. *Electrochem. Soc. Trans.* **2008**, *16*, 159–164.
12. Bachmann, J.; Jing, J.; Knez, M.; Barth, S.; Shen, H.; Mathur, S.; Gösele, U.; Nielsch, K. Ordered Iron Oxide Nanotube Arrays of Controlled Geometry and Tunable Magnetism by Atomic Layer Deposition. *J. Am. Chem. Soc.* **2007**, *129*, 9554–9555.
13. Fan, H. J.; Knez, M.; Scholz, R.; Hesse, D.; Nielsch, K.; Zacharias, H.; Gösele, U. Influence of Surface Diffusion on the Formation of Hollow Nanostructures Induced by the Kirkendall Effect: The Basic Concept. *Nano Lett.* **2007**, *7*, 993–997.
14. Banerjee, P.; Perez, I.; Henn-Lecordier, L.; Lee, S. B.; Rubloff, G. Nanotubular Metal−Insulator−Metal Capacitor Arrays for Energy Storage. *Nat. Nanotechnol.* **2009**, *4*, 292–296.
15. Peng, Q.; Sun, X. Y.; Spagnola, J. C.; Saquing, C.; Khan, S. A.; Spontak, R. J.; Parsons, G. N. Bi-directional Kirkendall Effect in Coaxial Microtuble Nanolaminate Assemblies Fabricated by Atomic Layer Deposition. *ACS Nano* **2009**, *3*, 546–554.
16. Rohan, J. F.; Casey, D. P.; Ahern, B. M.; Rhen, F.; Roy, S.; Fleming, D.; Lawrence, S. E. Coaxial Metal and Magnetic Alloy Nanotubes in Polycarbonate Templates by Electroless Deposition. *Electrochem. Commun.* **2008**, *10*, 1419–1422.
17. Bae, C.; Yoon, Y.; Yoo, H.; Han, D.; Cho, J.; Lee, B. H.; Sung, M. M.; Lee, M.; Kim, J.; Shin, H. Controlled Fabrication of Multiwall Anatase TiO_2 Nanotubular Architectures. *Chem. Mater.* **2009**, *21*, 2574–2576.
18. Abdel-Fattah, T.; Siochie, E.; Crooks, R. Pyrolytic Synthesis of Carbon Nanotubes from Sucrose on a Mesoporous Silicate. *Fullerenes, Nanotubes, Carbon Nanostruct.* **2006**, *14*, 585–594.
19. Scott, D. S.; Dullien, F. A. L. Diffusion of Ideal Gases in Capillaries and Porous Solids. *AIChE J.* **1962**, *8*, 113–117.
20. Lee, W.; Ji, R.; Gösele, U.; Nielsch, K. Fast Fabrication of Long-Range Ordered Porous Alumina Membranes by Hard Anodization. *Nat. Mater.* **2006**, *5*, 741–747.
21. Knez, M.; Nielsch, K.; Niinistö, L. Synthesis and Surface Engineering of Complex Nanostructures by Atomic Layer Deposition. *Adv. Mater.* **2007**, *19*, 3425–3438.
22. Lim, B. S.; Rahtu, A.; Gordon, R. G. Atomic Layer Deposition of Transition Metals. *Nat. Mater.* **2003**, *2*, 749–754.
23. Gu, D.; Tapily, K.; Shrestha, P.; Zhu, M. Y.; Celler, G.; Baumgart, H. Experimental Study of ALD HfO_2 Deposited on Strained Silicon-on-Insulator and Standard SOI. *J. Electrochem. Soc.* **2008**, *155*, G129–G133.